Recent Advances in RF Pulse Compressor Systems at SLAC

Sami G. Tantawi and Christopher D. Nantista

Stanford Linear Accelerator Center, 2575 Sand Hill Rd, Menlo Park, CA 94025

Abstract. We will review the design of the dual-mode X-band rf system proposed for the Next Linear Collider (NLC). Recent experimental data are presented. The system is to produce 400 ns pulses with power levels up to 600 MW. A proof-of-principle experiment is being constructed at SLAC. Four 50 MW klystrons will power a fully dual-moded resonance delay line pulse compression system. Both the transfer line and the delay lines are dual-moded. The modes carried by the transfer line are controlled by the rf phases of the different klystrons. The modes in the delay lines are controlled by a set of mode converters at the input and the end of each delay line. By manipulating the modes in the transfer line, one can achieve either no pulse compression or a pulse compression ratio of 4. The total output power will be 200 MW for 1.6 microseconds or 600 MW for 400 nanoseconds.

INTRODUCTION

Most proposed designs for future linear colliders contain long runs of waveguides. In X-band room temperature designs the total of these runs is on the order of 100 km or more. These waveguides are used for rf distribution and rf pulse compression. In particular, multi-bunch operation requires the rf pulse compression system to have a flat output pulse for a relatively long duration. Efficient production of such a flat pulse requires long waveguide delay sections. To minimize losses and enhance power handling capabilities, one must use overmoded waveguides. Manipulating rf signals in highly overmoded waveguide is not trivial. With even simple functions, such as bends, the designs are complicated by the need to ensure the propagation of a single mode without losses due to mode conversion to other modes.

To reduce the length of these waveguides we suggested multimoded systems [1]. In these systems the waveguide is utilized multiple times by carrying different modes. At first glance, one might think that this would lead to an additional complications in the design of most rf components. Indeed, one has to invent a whole new set of multimoded components. However, since manipulations such as bending an overmoded waveguide tend to couple the modes together anyway, it turns out that meeting the additional requirements of multimoded components can be rather simple. From the mechanical design point of view, most of these components are compact.

Here, we will review the design of the dual-mode X-band rf system proposed for the Next Linear Collider (NLC). Recent experimental data are presented. A proof-of-principle experiment is being constructed at SLAC. The total design output power is 600 MW for 400 nanoseconds.

CP691, *High Energy Density and High Power RF: 6th Workshop,* edited by S. H. Gold and G. S. Nusinovich

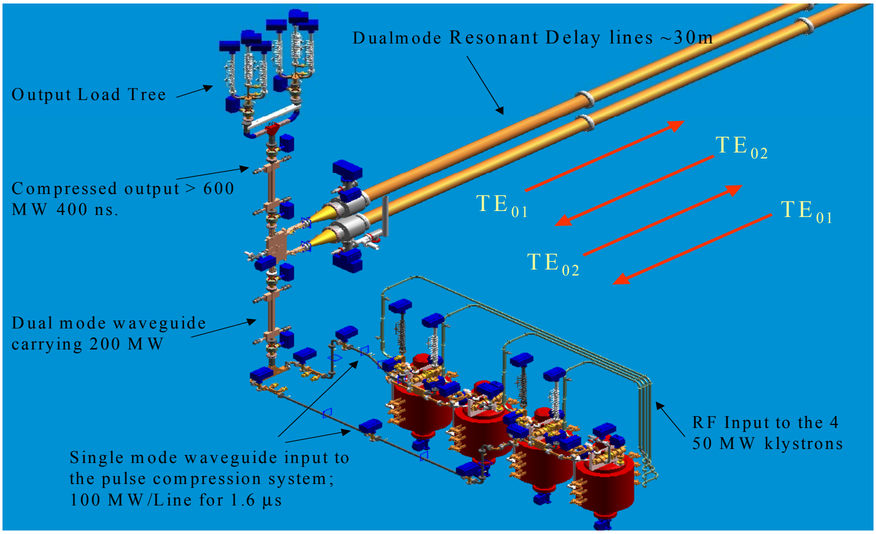

FIGURE 1. Layout of the of NLC proof-of-principle experiment.

SYSTEM DESCRIPTION

The system is shown in Fig. 1. Four 50 MW klystrons will power a fully dual-moded resonant delay line pulse compression system. Both the transfer lines and the delay lines are dual-moded.

The modes carried by the transfer lines are controlled via the relative rf phase between the two pairs of klystrons The modes in the delay lines are controlled by a set of mode converters at the input and the end of each delay line. By manipulating the modes in both the transfer lines one could achieve, no pulse compression or a pulse compression ratio of 4. The total output power is 200 MW for 1.6 microseconds and 600 MW for 400 nanoseconds.

We have adopted a general philosophy in our designs. Most of the manipulation of rf are made with planar components. These are rectangular waveguides with all manipulations made in the H-plane. Two modes are allowed to propagate – the TE_{01} and the TE_{02} modes. Because manipulations are only two-dimensional the height of the waveguide is a free parameter, which is used to reduce the field level and losses. In this system, we increased the height of most of the rectangular components to reduce the electric field level to approximately 45 MV/m. The waveguide cross-section is close to a square. We were careful not to increase the height more than necessary to avoid complications that result from an increased level of overmoding.

To transport the rf signal, we use circular waveguides. These carry the TE_{01} and TE_{11} modes. We connect between circular and rectangular waveguides using special, mode-preserving circular-to-rectangular tapers. These convert the TE_{10} rectangular mode into the TE_{11} circular mode and the TE_{20} rectangular mode into the TE_{01} circular mode. All vacuum functions, connection flanges and pumpout devices are implemented in circular waveguide. We also implement the diagnostic devices, i.e. mode-selective directional couplers, in circular waveguide.

The highly overmoded delay lines carry both the TE_{01} and the TE_{02} modes. Because these two modes have no axial wall currents the design of the connection flanges is simplified.

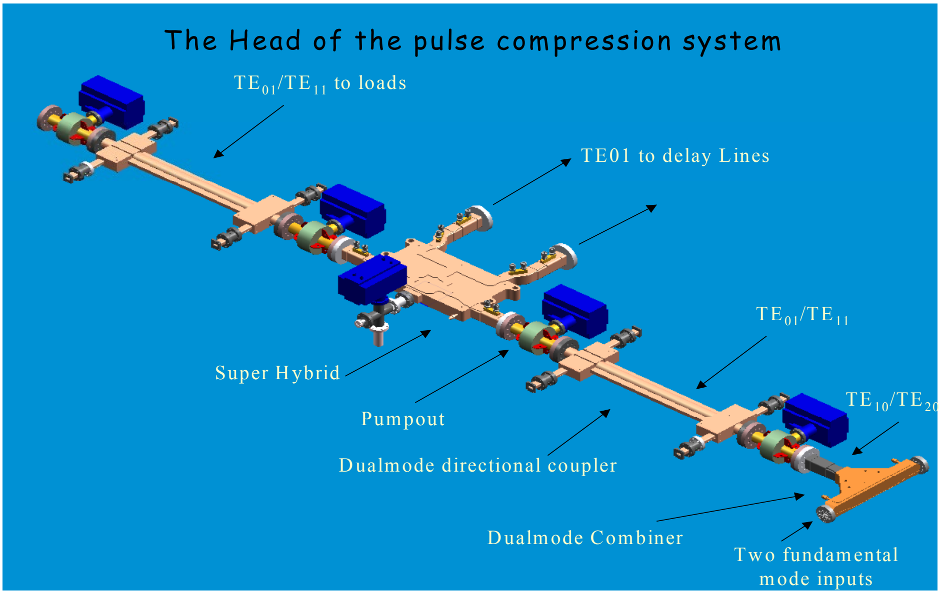

FIGURE 2. The dual-mode transfer line.

TRANSFER LINE

The design of the transfer line and the pulse compression head is shown in Fig. 2. The four klystrons are divided into two banks, each contains two klystrons. Each two klystrons are combined together to produce essentially a single rf source with an output power of 100 MW for 1.6 µs. These two 100 MW rf sources feed the combiner. The combiner launches two modes into the system. The weight of each mode is dependent on the relative phase and amplitude between the two banks of klystrons. The system is designed such that if the launched mode is the TE_{20} rectangular (TE_{01} circular), then the power is directed to the delay lines, and the compressed pulse is launched at the output towards the load tree in the same mode. On the other hand, if the launched mode is the TE_{10} rectangular (TE_{11} circular), the power is directed to the loads in that mode without pulse compression.

In the following we will present and describe each component in that line separately.

The Combiner

The combiner design, together with an HFSS illustration of its functionality, is shown in Fig. 3. The elongated post is designed to match the TE_{10} mode without affecting the match of the TE_{20} mode at the T-junction.

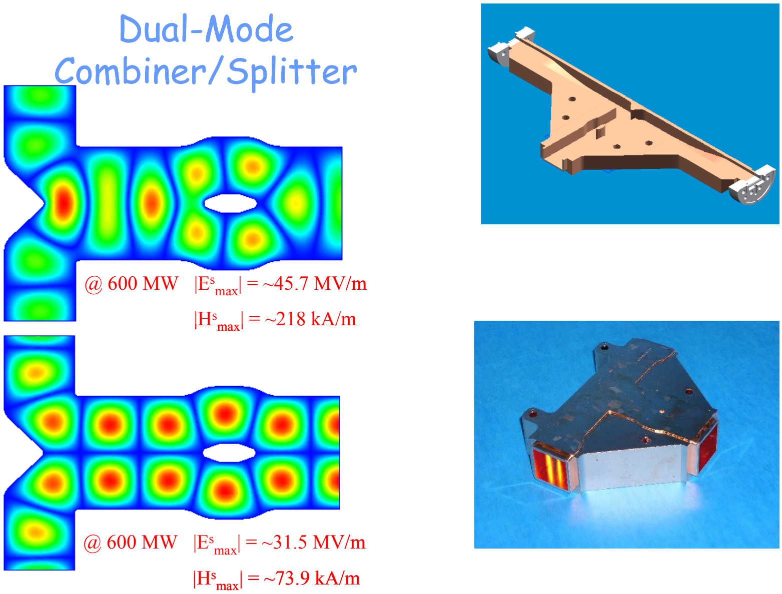

FIGURE 3. The dual-mode combiner/splitter design.

Circular-to-Rectangular Taper

Figure 4 shows the design of the circular-to-rectangular taper, together with HFSS simulation results.

To test the functionality of this taper combined with the splitter, we connected the two together as shown in Fig. 5. The TE_{01} mode is launched through the circular part of the taper using a wrap-around mode converter [2]. The output of the taper then launches the TE_{20} mode in the symmetry port of the combiner. The signal is split equally out the remaining two ports. We measured this signal through a specially designed set of instrumental height and width tapers, which reduces the waveguide cross-section to the standard size, connectable to the network analyzer.

The results of these measurements are shown in Figs. 6a and 6b. From Fig. 6a one can estimate the total losses of the combiner, the circular to rectangular taper, the wraparound mode converter, and the instrumental tapers to be about 1.3%. Because of the asymmetry of the TE_{20} mode, one should observe a π phase difference between the two ports. Within the measurement and fabrication tolerances, this is verified in the experimental data shown in Fig. 6b.

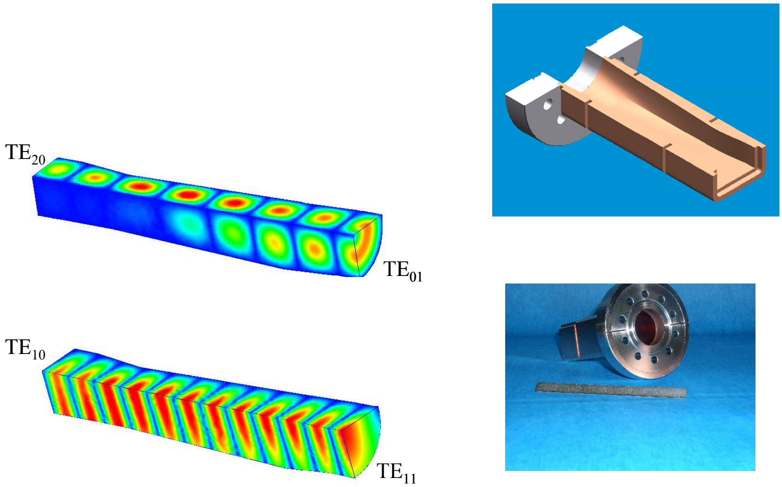

FIGURE 4. Dualmode circular-to-rectangular taper.

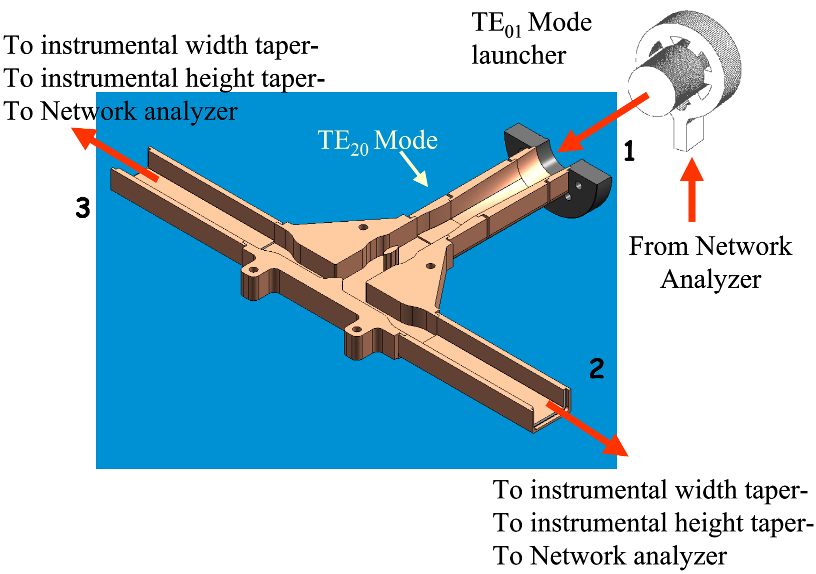

FIGURE 5. Cold test setup for the combiner and circular-to-rectangular taper.

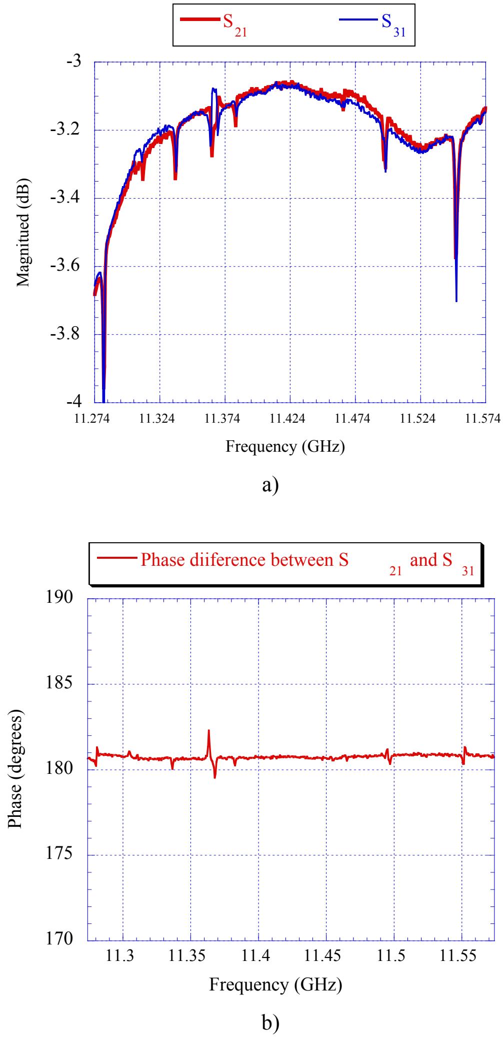

FIGURE 6. Cold test results of: splitter – circular-to-rectangular taper – wrap-around mode converter – instrumental height taper – instrumental width taper. Total losses at 11.424 GHz =1.3%. a) Magnitude, b) Phase.

The Pumpout

Figure 7 shows the structure of the 1.6”-diameter circular pumpout. The number of holes around the azimuth is greater than the maximum azimuthal variation for any mode that can propagate in this waveguide. The distances between the rows of holes are adjusted to cancel any reflection for both utilized modes. Figure 8 shows the measured transmission for each mode.

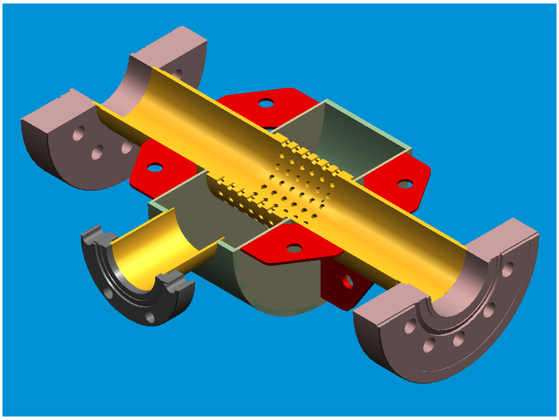

FIGURE 7. Pumpout design. The set of holes are designed to cancel any coupling or self-coupling for the TE_{01} and the TE_{11}.

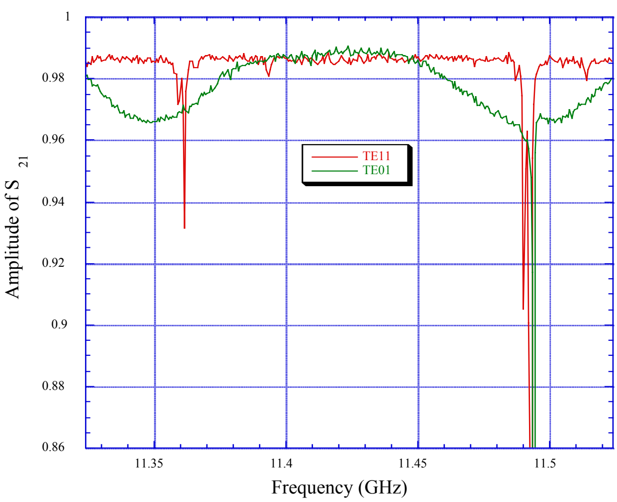

FIGURE 8. Cold Test Results of the dualmode pumpout.

Dual-Mode Directional Coupler

The design of the dual-mode directional coupler is shown in Fig. 9. Two waveguides are coupled through a set of holes to the main circular waveguide. To couple the TE_{01} circular mode the width of one rectangular waveguide is adjusted to match the phase velocities. Because the circular waveguide is overmoded and the fundamental TE_{11} mode has a phase velocity close to the speed of light, one cannot match this velocity in a single moded rectangular waveguide. To match the velocities we had to use a ridge waveguide.

To make the coupler directional and to discriminate against coupling of unwanted modes, the coupling hole pattern was chosen to represent a Hamming window. Finally, one has to bend the rectangular and ridge waveguide so that one can connect vacuum windows and diagnostic devices. These bends double as tapers to standard size rectangular waveguide, WR90 in our case. The proper matching of these bends and the attached vacuum window is crucial for the maintaining good directivity.

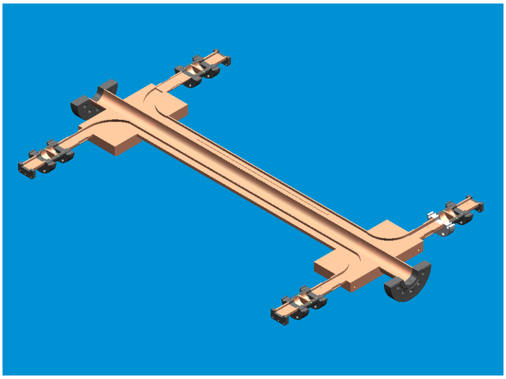

FIGURE 9. Dual-mode directional coupler for system diagnostics.

In Figure 10, we show the coupling to the TE_{11} arm due to an injected TE_{01} mode. Knowing that the coupling to the TE_{01} arm is –47 dB, one estimates a minimum isolation of –45 dB. The dynamic range of our equipment limited these measurements. In Fig. 11 the directivity of the TE_{01} mode arm is shown. The matching section at the end of the coupler, including the vacuum windows, limits the directivity.

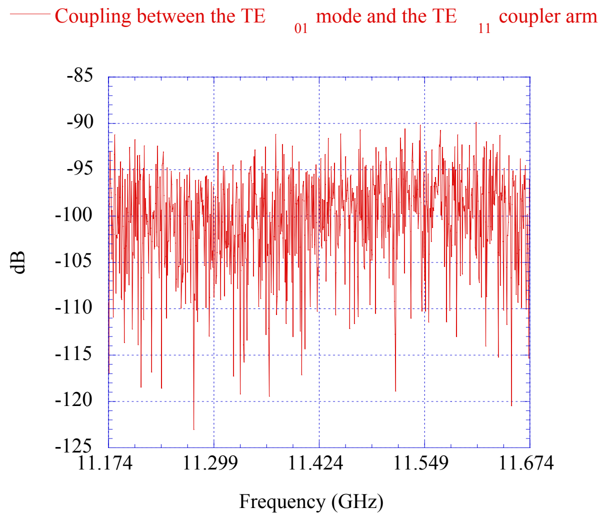

FIGURE 10. Coupling of TE_{01} to the TE_{11} arm. The dynamic range of the equipment limits the measurement.

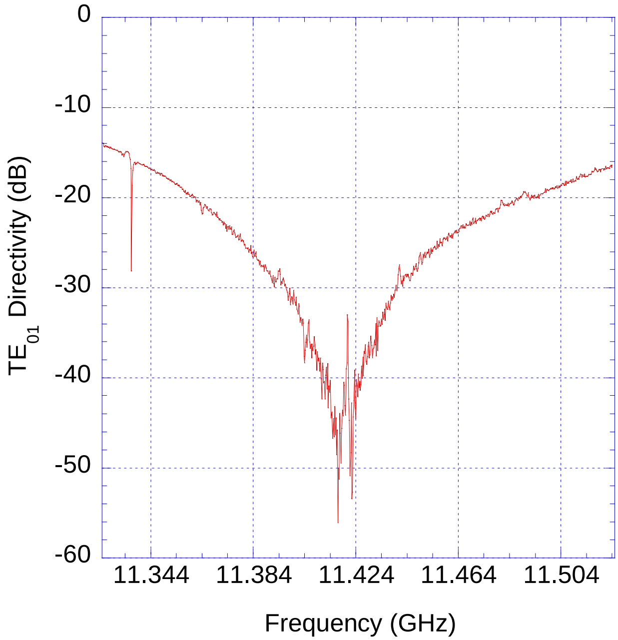

FIGURE 11. Measured directivity of the TE_{01} arm.

The Superhybrid

The heart of the pulse compression system is shown in Fig. 12. An illustration of its functionality is shown in Fig. 13. When the injected mode is TE_{10} (TE_{11} circular), the signal passes through. When the injected mode is TE_{20} (TE_{01} circular) the signal is sent to the delay lines and the compressed pulse is sent to the output.

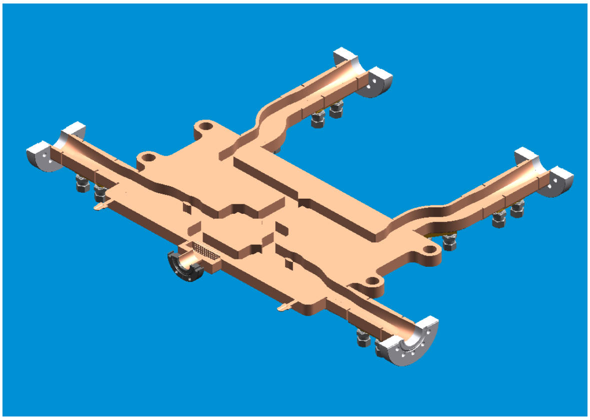

FIGURE 12. Superhybrid design: basically three planer hybrids on one single substrate.

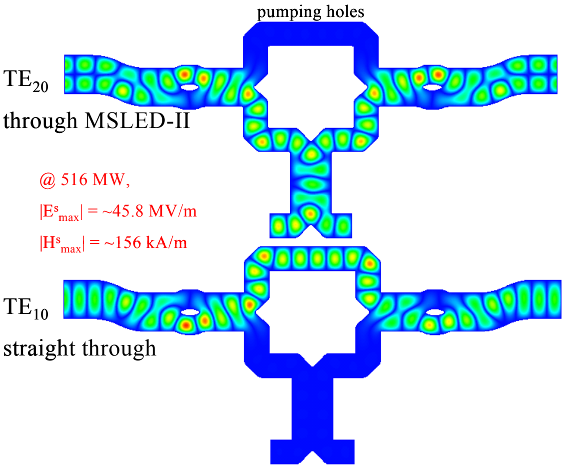

FIGURE 13. Superhybrid simulations.

By shorting the ports that should connect to the delay lines (see Figs. 1 and 2) one can measure the transmission of the TE_{01} mode (TE_{20} mode in the rectangular guides) through the system. These measurements are shown in Fig. 14. With the exception of spurious mode resonances, the system has excellent power transfer characteristics.

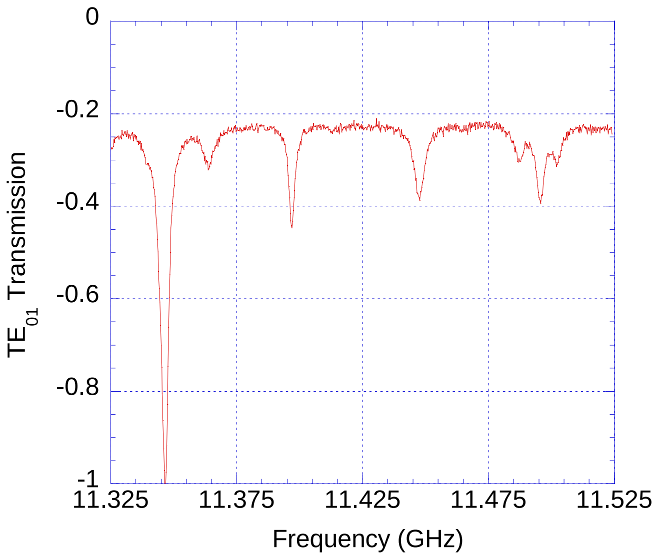

FIGURE 14. Measured response of the superhybrid when excited with the TE_{01} mode.

Similarly, Fig. 15 shows the response of the system when excited with the TE_{11} mode in the circular guide. Again, with the exception of spurious mode resonances, which depend mainly on the mode transducers at either end of the device, the measurements show excellent transfer characteristics. The boundary conditions at the delay line ports do not affect these measurements.

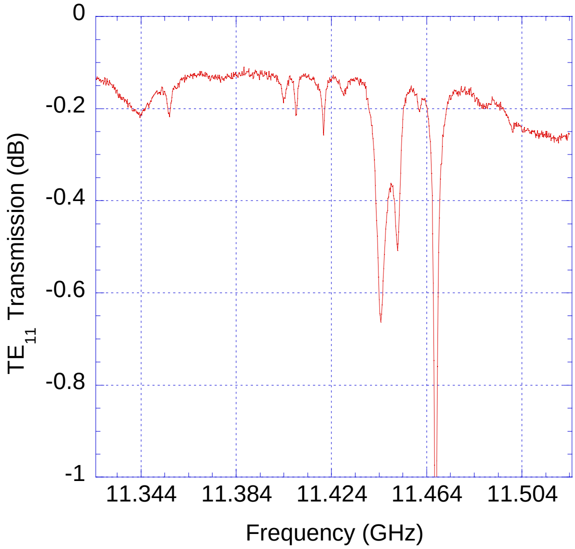

FIGURE 15. Measured response of the superhybrid when excited with the TE_{11} mode.

THE DUAL-MODE LOAD SYSTEM

To dump the output power, one needs a load that accepts both the TE_{01} mode and the TE_{11} mode. This is accomplished by using a splitter similar to the combiner shown above. First the power in either mode is split into two arms as shown in Fig. 16.

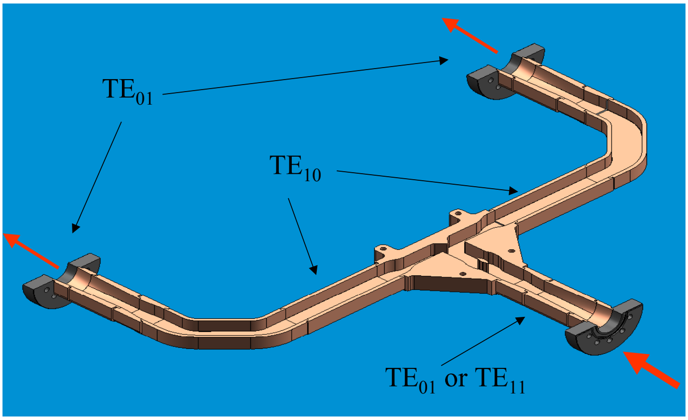

FIGURE 16. Dual-mode Splitter: Irrespective of the incident mode, the power is split in two and the two outputs launch the TE_{01} mode.

After the power is split in half, the power in each arm is further split into four different waveguides using the splitter shown in Fig. 17. We end up with the power being divided into eight standard waveguides. These waveguides are terminated with all-metal, fundamental-mode loads, which are water cooled.

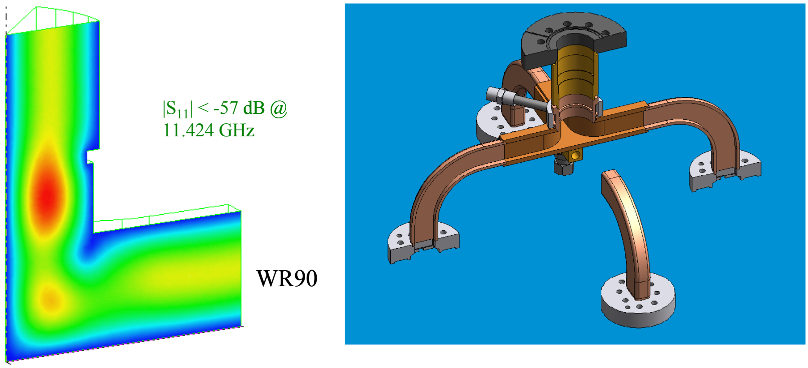

FIGURE 17. Four-way splitter design.

THE DUAL-MODE DELAY LINE

Consider the delay line shown in Fig. 1. The rf signal is injected into the delay line waveguide in the TE_{01} mode. This is the only azimuthally symmetric TE mode supported at the input port. The waveguide is then tapered up to a diameter that supports several TE_{0n} modes. The TE_{01} mode travels all the way to the end of the delay line and then gets reflected and converted into the TE_{02} mode. The TE_{02} mode travels back to the beginning of this line and, since the input of the line cuts off this mode, gets reflected. If the input taper is designed carefully, TE_{02} can be reflected perfectly, without mixing. Then, because of reciprocity, the TE_{02} wave gets converted back to TE_{01} at the end of the line. Finally, this mode travels back and exits the line. The total delay in the delay line is approximately twice that seen by a single moded line. Hence, one can cut the length of delay line by a factor of two.

The mode converter at the end of the delay line can be seen in Fig. 18. It is basically a step in the circular waveguide. If the big waveguide at its input supports only the TE_{01} and TE_{02} modes among all TE_{0n} modes and the small waveguide supports only the TE_{01} mode, then the device could be viewed as a three-port network. One can choose the diameter of the small guide such that the couplings between each mode in the large guide and the single mode in the small guide are equal. In this case, it is a symmetrical three-port network. A theory for such a device is presented in [3]. It shows that there exists a position for placing a short circuit in the middle arm of this three-port network (the small guide in this case) that makes it possible to transfer the power perfectly between the remaining two arms, or in this case between the TE_{01} and the TE_{02} modes in the large guide.

The only step left in the design of this end mode converter is a careful taper design that reduces the diameter of the delay line into the diameter of a waveguide that can support only TE_{01} and TE_{02}. The taper needs to transfer both modes perfectly. We made the compact taper by a computer-optimized series of steps as shown in Fig. 18. A similar design has been implemented for the input taper, which transfers the TE_{01} mode perfectly and reflects the TE_{02} mode without any mode conversion to other TE_{0n} modes.

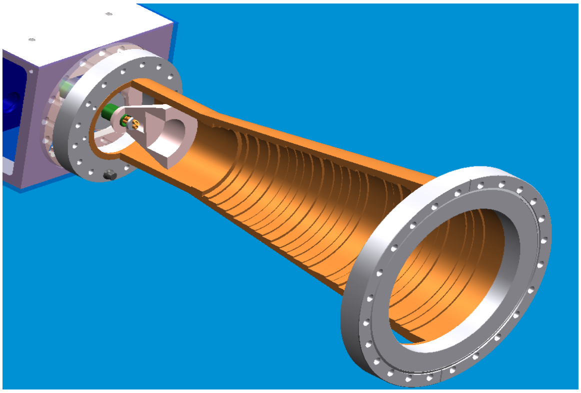

FIGURE 18. End taper and mode converter. The movable cup at the end of the taper reflects the TE_{01} mode into the TE_{02} mode, and vice versa.

Using this delay line, we implemented a dual-moded version of the so-called SLED-II pulse compression system [4]. We simply added an iris at the beginning of delay line. The performance of this pulse compression system is shown in Fig. 19. The compression ratio, defined as the ratio between the input pulse width and the delay time in the line, is 4. The power gain is close to 3.2.

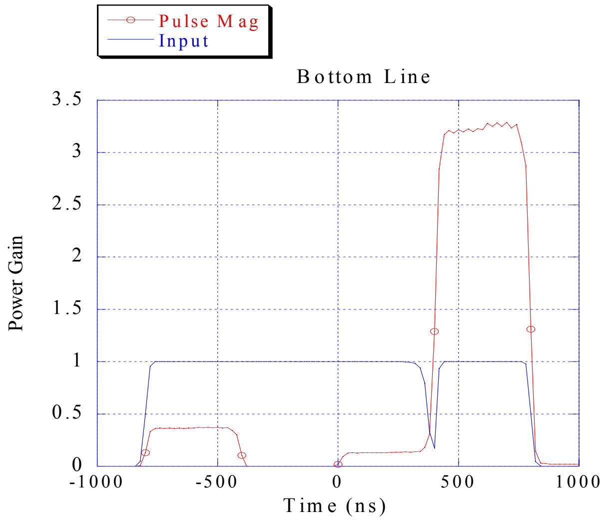

FIGURE 19. Measured time response of one of the dual-moded delay lines. The phase of the input signal is flipped by a 180° during the last 400 ns.

ACKNOWLEDGMENTS

This work is a result of a continuous effort by many researchers and engineers over many years. In particular, the efforts of N. Kroll, R. Miller, P. Wilson, V. Dolgashev, K. Fant, C. Pearson, and R. Ruth were instrumental to the results achieved to date. We wish also to thank Jose Chan for his persistent efforts during the manufacturing and testing of components. This work was supported by the U.S. Department of Energy under contract DEAC03-76SF00515.

REFERENCES

1. S.G. Tantawi *et al.*, “A Multimoded RF Delay Line Distribution System for the Next Linear Collider,” *Phys.Rev.ST Accel. Beams*, vol. 5, March 2002.
2. S.G. Tantawi *et al.*, "The Generation of 400-MW RF Pulses at X Band Using Resonant Delay Lines," *IEEE Trans. Microwave Theory Tech.*, vol. 47, no. 12, pp. 2539-2546, Dec. 1999; SLAC-PUB-8074.
3. Sami G. Tantawi, Ronald D. Ruth, Arnold E. Vlieks, and Max Zolotorev, “Active high-power RF pulse compression using optically switched resonant delay lines,” *IEEE Trans. Microwave Theory Tech.*, MTT-45(8), August 1997, p. 1486–1492.
4. P.B. Wilson, Z.D. Farkas, and R.D. Ruth, “SLED-II: A New Method of RF Pulse Compression,” presented at the Linear Accelerator Conf., Albuquerque, NM, September 10-14, 1990.